CHAPTER VIII

IMPACT OF SURFACE DEFECT (Ti^{3+}) PRESENT IN TiO_2 ON CATALYTIC PROPERTIES OF THE Co/TiO_2 CATALYST

The hydrogenation of CO and related reactions on reducible oxide-supported noble metals are sensitive to metal–support interaction [91]. As known, Co/TiO_2 catalyst is considered to have strong metal support interaction [92-96] and shows high activities in CO hydrogenation. Co/TiO_2 is known to give a distribution of FT products ranging from C1 to C18+ hydrocarbons with high selectivity for C2-C11[97].

The interaction between a support and a metal oxide (catalyst) precursor is an important factor used to determine the dispersion of a metal catalyst and hence the behavior of a catalyst as well [97]. In fact, the synthesis of highly dispersed cobalt catalysts requires the initial formation of very small CoO or Co_3O_4 crystallites. It was reported that the formation of small oxide clusters needs strong interactions between the support and the cobalt precursor. However, too strong interaction would suppress reduction of these CoO_x clusters resulting in low reducibilities. Moreover, strong interaction between Co and TiO_2 can produce the suboxide at interface that is more resistant to reduction than the other supports [98].

The absence of bulk oxygen vacancy defects in the TiO_2 markedly reduces the extent of interface chemistry leading to negligible reduction at the metal/TiO_2 interface to form suboxide (Co/TiO_x; $x<2$). It appears that the diffusion of oxygen vacancy defects from the bulk to the interface is a key driving force in the process of suboxide formation [99]. In case of surface defect site, it revealed that metal/TiO_2 formed strong metal-TiO_2 bond. The bond energy for the metal is larger at the oxygen defect site than at the normal site on the titania surface [100].

In this work, effect of surface defect of titania support on characteristics and activity of Co/TiO_2 catalyst in methanation was investigated. Titania support was prepared by sol-gel and then calcined under N_2 plus increasing amount of O_2 to change the surface defect concentration. Co/TiO_2 was prepared by the incipient wetness impregnation of 20 wt% cobalt onto prepared titania. CO_2-TPD and ESR were used as probe monitor for showing defect site on titania surface. TPR and H_2-chemisorption were used to identify basic properties of Co/TiO_2 catalyst and investigate activity of Co/TiO_2 using CO hydrogenation. In case of morphology, element distribution of Co/TiO_2 and crystallite size of TiO_2 support, they were analyzed using SEM, EDX and XRD, respectively. The nomenclature used for the catalyst samples in this study is following:

- $TiO_2(X)$: the calcined titania support with X% by volume of O_2 in feed during calcinations.
- $Co/TiO_2(X)$: the titania-supported cobalt catalyst with X% by volume of O_2 in feed during calcination of titania support.

8.1 Determination of Ti^{3+} on titania

The surface area and crystallite size of prepared titania at various calcinations conditions is shown in Table 5.1. Surface areas of titania were found to decrease with increasing the amount of oxygen in feed during calcination of titania percent whereas crystallite size was apparently constant. Thermal desorption spectra of CO_2 from a titania surface is shown in Figure 5.2. It revealed that the surface Ti^{3+} increased with $\%O_2$ in nitrogen. Based on ESR analysis as shown in figure 7.5, it showed that surface of titania has more defect when increasing $\%O_2$ during calcination process as also seen from CO_2-TPD.

8.2 Cobalt dispersion on TiO_2-supported cobalt

XRD patterns of Co/TiO_2 catalyst is shown in Figure 8.2. It revealed that Co/TiO_2 catalysts in this work exhibited mainly two patterns; Anatase titania and Co_3O_4 formed after calcinations. XRD patterns of titania showed strong diffraction peaks at 26°, 37°,

48°, 55°, 56°, 62°, 69°, 71° and 75° indicating titania in the anatase form. After calcination, the diffraction peaks of Co_3O_4 at 36°, 46° and 65° can be observed. Jongsomjit et al. [101] reported XRD peaks of $CoTiO_3$ at 23°, 32°, 35°, 49°, 52°, 62° and 64°. Kraum et al. [102] reported the observation for XRD peaks of $CoTiO_3$ phase along with Co_3O_4 on the calcined Co/TiO_2 catalyst using cobalt (III) acetyl acetonate as a precursor for cobalt. They suggested that the formation of $CoTiO_3$ by the use of cobalt (III) acetyl acetonate as a precursor can be attributed to the migration of cobalt ions into the support lattice, with the consecutive formation of titanate. However, based on differences in the cobalt precursor, the amounts of cobalt loading and the calcinations condition used in the present study, the formation of $CoTiO_3$ was not observed in the calcined Co/TiO_2 catalyst in this present study.

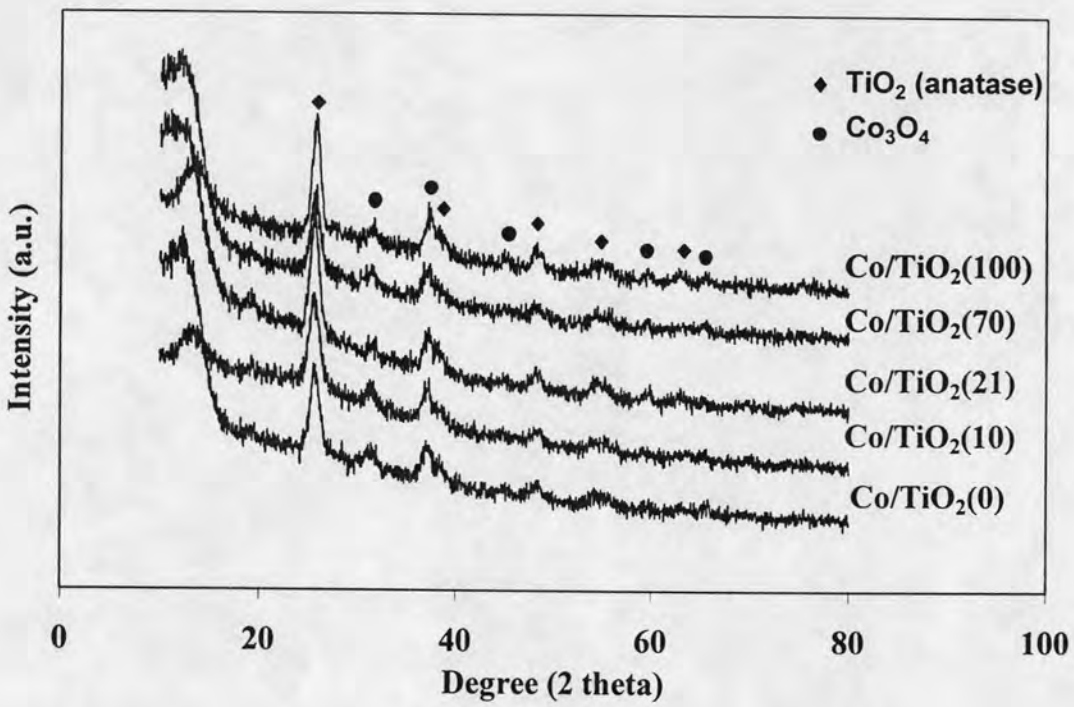

Figure 8.2: XRD patterns of Co/TiO_2 catalyst

Amount of H_2-chemisorption on the reduced Co/TiO_2 is shown. It revealed that amounts of H_2-chemisorption increased with increasing $\%O_2$ in feed during alcinations of TiO_2 up to 21% and then constant with higher amount of O_2 used. The evaluation of metal dispersion is a difficult task and requires very careful interpretation of the data

obtained from different techniques (e.g. H_2-chemisorp, XPS, XRD), which yield different pieces of information on the particles of cobalt. H_2-chemisorption gives a measure of the number of reduced cobalt metal surface atoms. However, H_2-chemisorption is unable to detect any cobalt that is chemically bonded to the support, either through the formation of a surface compound or through strong metal-support interaction. The latter phenomenon is understood to entail an electron exchange between a partially reduced support and the metal and leads to the suppression of hydrogen chemisorption. Moreover, strong metal-support interaction has been found to affect the metal dispersion [103].

As seen in table 8.1, surface area and %Co dispersion which the latter was calculated from amounts of H_2-chemisorption on Co/TiO_2. It was found that % Co dispersion increased with increasing $\%O_2$ in feed during calcinations of TiO_2 up to 21% in nitrogen and then constant. Shouli et al. [98] reported that the synthesis of highly dispersed cobalt catalysts required strong interactions between the support and the cobalt precursor. Wei-xing et al. [104] indicated that the bond energy for the metal and titania is larger at the oxygen defect site than at the normal site on the titania surface. From CO_2-TPD, ESR and H_2-Chemisorption results, it was observed that increasing of surface defect of supported titania affected to strong interaction behavior between Co and titania. Because of increasing Ti^{3+} present, % Co dispersion on titania increased.

Table 8.1: Characteristics and CH_4 selectivity of prepared Co/TiO_2

	sample				
	$Co/TiO_2(0)$	$Co/TiO_2(10)$	$Co/TiO_2(21)$	$Co/TiO_2(70)$	$Co/TiO_2(100)$
surface area (m^2/g)	55	51	51	52	50
H_2-chemisorption (10^{-6} mol/g)	1.6	1.9	2.7	2.8	2.8
% Co dispersion[a]	0.09	0.11	0.16	0.16	0.16
% reducibility[b]	35	48	51	61	66
CH_4 selectivity (%)[c]	99	99	99	99	99

[a] Calculated from the amount of H_2-chemisorption. [b] Calculated from TPR. [c] Calculate from CH_4 selectivity (%) = (mole of CH_4/mole of total product) × 100.

SEM and EDX were performed to study the morphologies and elemental distribution of the catalyst samples, respectively. There was no significant change in morphologies of catalyst samples upon the presence of Ti^{3+} in TiO_2. The elemental distributions can be clearly seen by EDX. The typical elemental distribution for Co/TiO_2 in nitrogen is shown in Figure 8.3. The distribution of cobalt, titanium and oxygen were well dispersed throughout the catalyst. Figure 8.4 and 8.5 show the typical elemental distribution for catalyst at 21% O_2 and 100% O_2 in nitrogen, respectively. According to oxygen distribution as seen from Figures 8.3 to 8.5, it can be observed that Ti^{3+} (oxygen vacancy site) increased with increasing of $\%O_2$ during calcination process of titania.

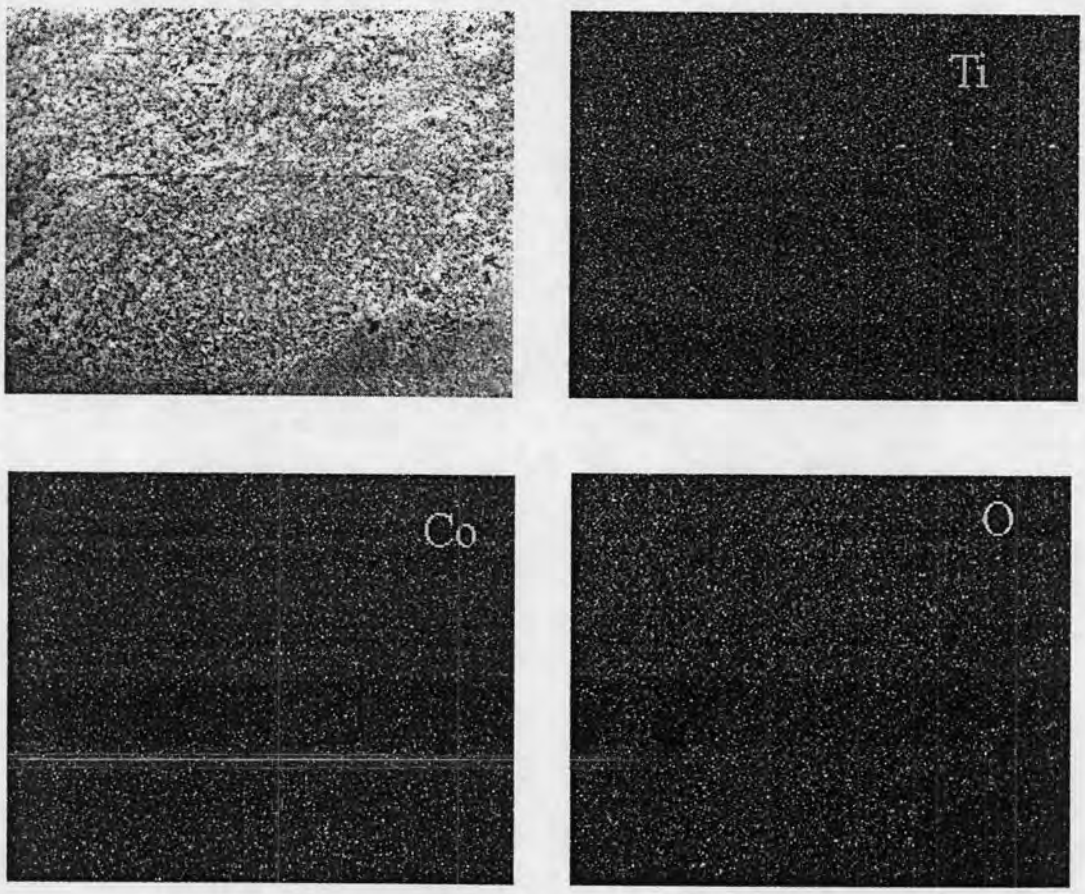

Figure 8.3: SEM micrograph and EDX mapping of $Co/TiO_2(0)$ at 600x

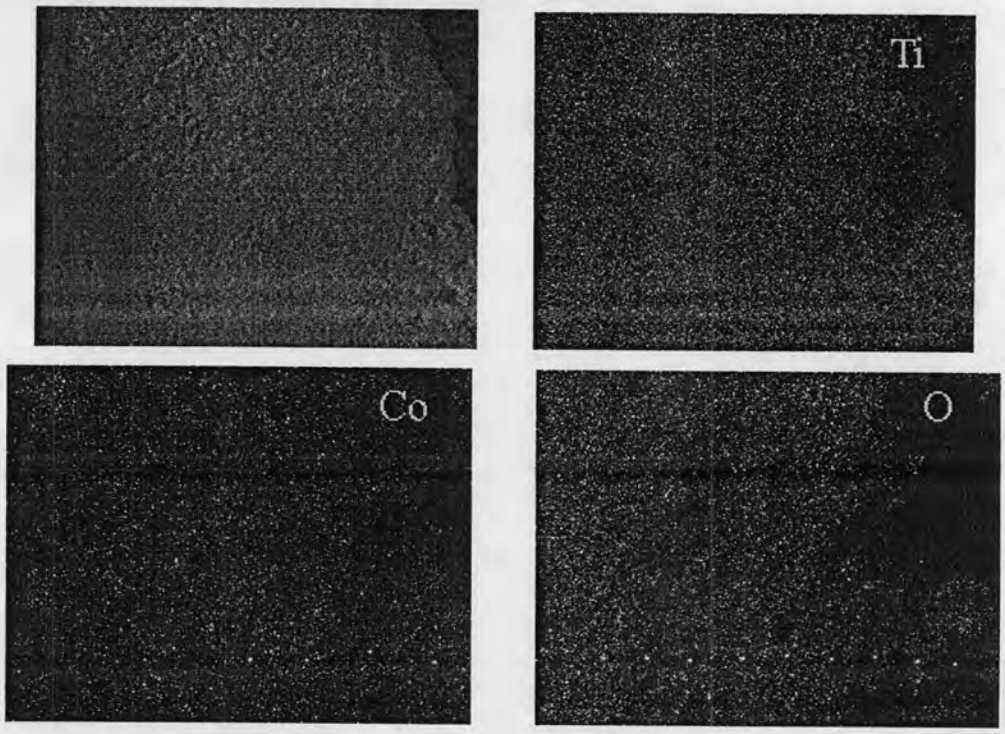

Figure 8.4: SEM micrograph and EDX mapping of $Co/TiO_2(21)$ at 600x

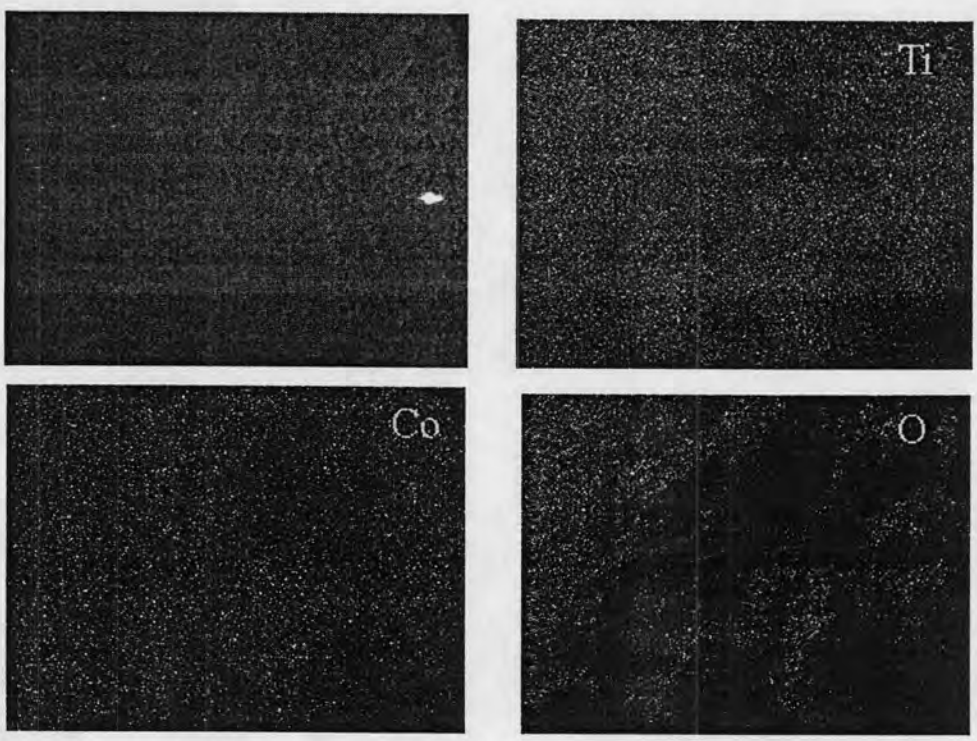

Figure 8.5: SEM micrograph and EDX mapping of $Co/TiO_2(100)$ at 600x

8.3 Reduction behaviors on TiO_2-supported cobalt

The TPR profiles of Co-supported titania are showed in figure 8.6. It indicated one reduction peak at ca. 723 K. Kraum et al. [102] concluded that only one broad peak exists for the reduction of Co_3O_4, which was assigned to the stepwise reduction of cobalt oxide via $Co^{3+} \rightarrow Co^{2+} \rightarrow Co^0$. This broad peak could result from an overlap of both reduction steps; no single steps could be derived where organic precursors were used. Two reduction steps of Co_3O_4 were showed in following equation

$$Co_3O_4 + H_2 \rightarrow 3CoO + H_2O \qquad (8.1)$$

$$CoO + H_2 \rightarrow Co^0 + H_2O \qquad (8.2)$$

Jongsomjit et al. [101] showed TPR profiles of bulk Co_3O_4, only one strong reduction peak at ca. 400°C can be observed for bulk Co_3O_4 which this peak can be assigned to the overlap of two-step reduction of Co_3O_4. It should be noted that the reduction peak for all samples were higher than that of bulk Co_3O_4. This might be due to at least three causes: (i) the particle size of the metal oxide in CoO/support is smaller than the particle the particle size of bulk Co_3O_4. The TPR profile of the titania support (not shown) showed no reduction peak. The smaller particle size is possibly more difficult to reduce than the larger one, (ii) some cobalt oxide and cobalt support interaction exists in the Co/support and (iii) some species which is different from Co_3O_4 is present [105].

The reducibility of Co/TiO_2 is also shown in Table 8.1. It revealed that % reducibility increased with $\%O_2$ in feed during calcinations of TiO_2. Based on the resulted H_2-chemisorp and TPR, it showed that the presence of Ti^{3+} on supported titania do not inhibit reduction of cobalt oxide from Co^{3+} to Co^0 by strong interaction behavior between support and catalyst. In contrary, the presence of Ti^{3+} in titania can enhance the % reducibility and cobalt dispersion of Co/TiO_2.

As seen from TPR profiles of Co/TiO_2, on the other hand, considering the case of 10% and 0% O_2 in nitrogen, it showed that reduction peaks were shifted to high temperature. This result may come from effect of inorganic and organic residual on

titania particle in form of impurity which occurred at low oxygen percent during alcinations process. This impurity was a main reason to induce the formation of suboxide in catalyst.

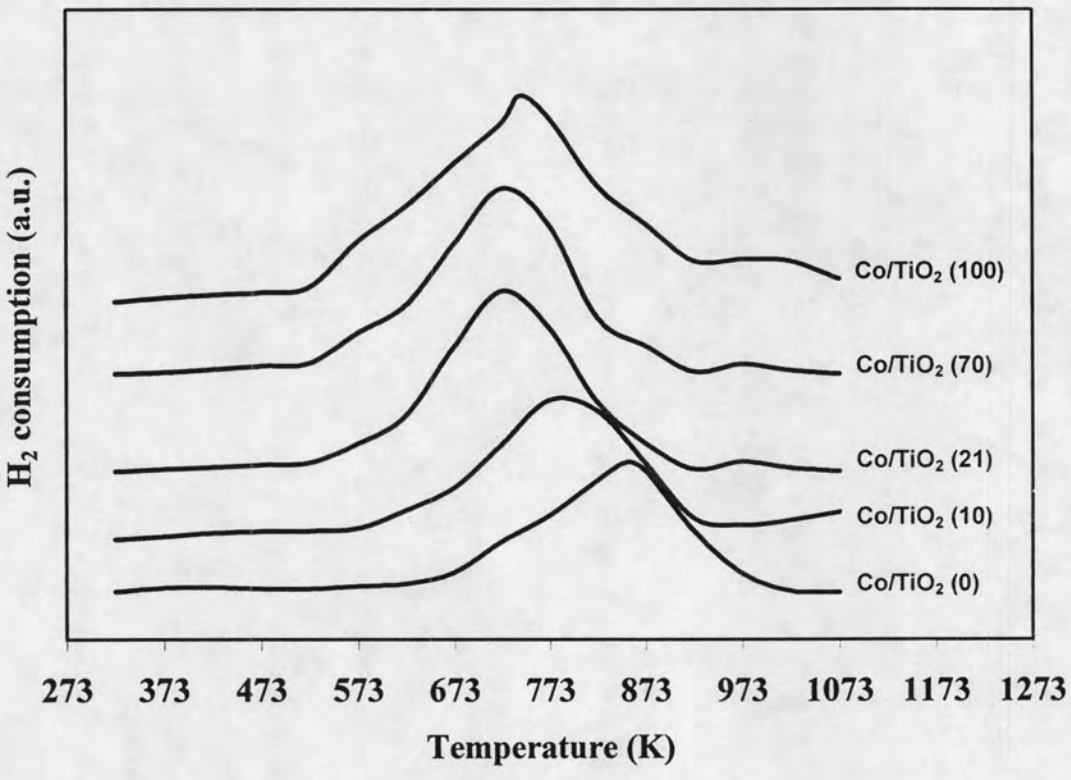

Figure 8.6: TPR profiles of the Co/TiO_2 with various TiO_2 calcined at different $\%O_2$ in feed during calcination process

8.4 Activity of TiO_2-supported cobalt catalysts during CO hydrogenation

CO hydrogenation is a means to convert synthesis gas obtained from natural gas reforming and coal gasification, into mainly desirable long chain hydrocarbons. The main reactions of CO hydrogenation are:

$$CO + [1+(m/2n)]H_2 \rightarrow (1/n)C_nH_m + H_2O \quad (a)$$

$$CO + 3H_2 \rightarrow CH_4 + H_2O \quad (b)$$

$$CO + H_2O \rightarrow CO_2 + H_2 \quad (c)$$

$$2CO \rightarrow C + CO_2 \quad (d)$$

An equation (a) is the formation of hydrocarbons higher than C1, and the equation (b) is methanation. The water-gas shift reaction, which is undesirable for natural gas conversion, is shown in equation (c). The Boudouard reaction, which results in carbon deposition on the catalyst surface, is shown in equation (d). Depending upon the type of catalyst used, promoters, reaction conditions (pressures, temperatures and H_2/CO ratios) and type of reactors, the distribution of the molecular weight of the hydrocarbon products can be noticeably varied. From this work, it was showed that five Co/TiO_2 samples showing in methanation. CH_4 selectivity of five Co/TiO_2 samples was shown in Table 2. Feller et al. [106] performed FTS in a down flow bed reactor at 463 K and 0.5 MPa. Co/SiO_2 (1g) was loaded into reactor with a flow rate of H_2: CO = 2:1. It found that CH_4 selectivity was about 14 %. It revealed that difference of nature of support and low H_2/CO ratio made the lower CH_4 selectivity. From results of Coville et al. [97], FTS was then performed at 523 K and 0.8 MPa pressure, using a H_2: CO ratio of 2:1. Co/TiO_2 (2g) was used in reaction. It was found that Co/TiO_2 gave a distribution of FT products ranging from C1 to C18+ hydrocarbon with high selectivity for C2-C11. Therefore, it showed that high H_2 : CO ratio in this work was the main cause of CH_4 production in methanation.

Entrained bed reactors or slurry bubble column reactors are better than fixed-bed reactors for CO hydrogenation since they can remove heat from this exothermic synthesis, allowing better temperature control. However, this work uses only small amount of catalyst sample along with high reactant flow rate. Therefore, diffusional limitations from mass and heat transfer can be negligible. In this work, a relatively high H_2/CO ratio was used to minimize deactivation due to carbon deposition follow equation (d) during reaction.

High reduction degree and high cobalt metal dispersion are considered to be two of the most important factors for CO hydrogenation catalysts. From above discussion, cobalt dispersion and reducibilities of titania-suppoted Co was found to be larger when higher amounts of Ti^{3+} on surface titania. As a result, high conversion of CO in methanation can be observed in case of high amounts of Ti^{3+} on surface titania as shown in Figure 8.7.

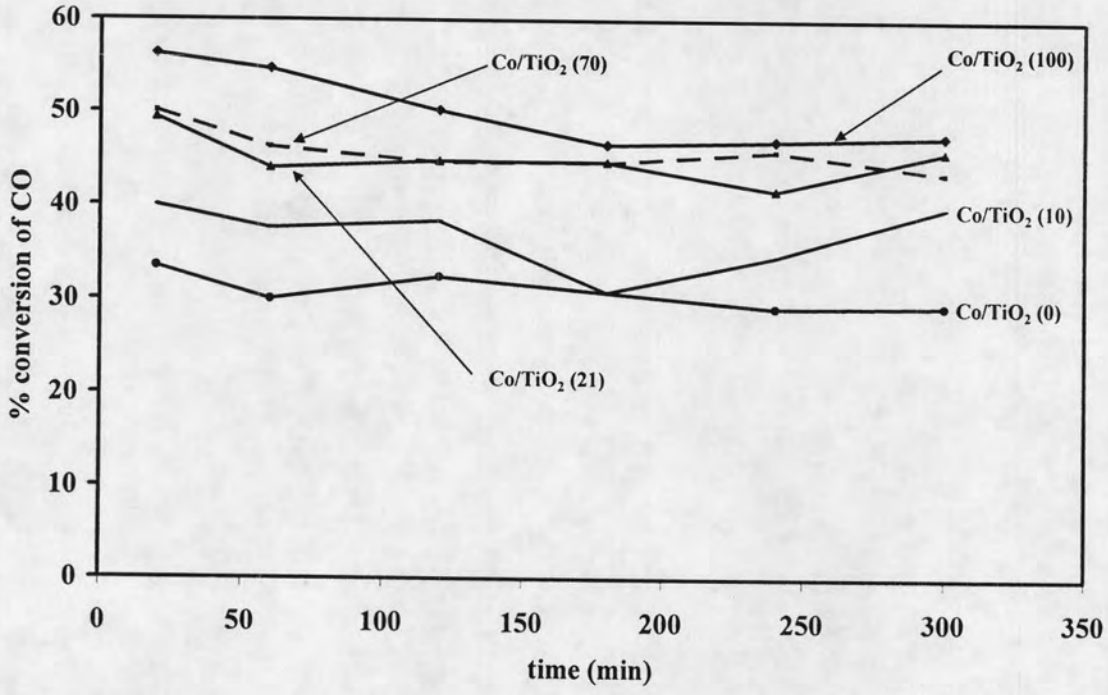

Figure 8.7: Time-on-stream behavior of Co/TiO_2 samples in methanation